CONTINUOUS-FLOW ELECTROPHORETIC SEPARATION OF BIOMOLECULES IN A TWO-DIMENSIONAL CAPILLARY-WELL MOTIF

*Lian Duan, Xiaoxing Xing, and Levent Yobas**
The Hong Kong University of Science and Technology, Hong Kong, S.A.R., P.R. CHINA

ABSTRACT

A two-dimensional (2D) capillary-well (CW) motif is a novel structure featuring thousands of cylindrical glass capillaries in diameter 100 and 600 nm and integrated through low-resolution photolithography (~2 μm) and standard silicon processing techniques. Owing to high entropic energy barriers imposed at capillary openings, this design offers a rapid high-performance sieving of biomolecules under intense electric fields as demonstrated here for continuous-flow DNA or protein electrophoresis.

INTRODUCTION

The size-dependent separation of macromolecules is of great significance in genomics, proteomics and clinical diagnostics [1]. Gel electrophoresis is the most commonly used technique and separates DNA fragments or proteins based on their size and charge. However, this method is time consuming and suffers from poor efficiency due to irregular pores throughout cross-linked gel structures [2]. The notion of replacing disordered gelatinous materials with highly ordered microfabricated structures could advance the separation performance [3]. Accordingly, various sieve structures have emerged to date including a microfabricated post array [4], nanowires [5], and a slit-well motif [6], toward accelerating separation analysis while maintaining an increased resolution. Nevertheless, many of these designs can only offer analysis at a low sample throughput due to batch operation and face challenges in sample recovery. These shortcomings limit the use of such innovative structures as a front-end sample preparation module for an integrated bioanalysis system.

In recent years, researchers have made notable advance in reducing the separation time while enhancing the throughput. Cox and co-workers fabricated an array of micro-scale posts and achieved continuous fractionation of large DNA molecules based on biased reorientation mechanism under an asymmetric pulsed electric field [7]. Based on the same mechanism, Zeng *et al.* made use of a large-area colloidal array and realized continuous-flow separation of DNA coils [8]. These studies, however, fell short of sieving small macromolecules such as proteins and rod-like DNA strands. Fu *et al*. addressed this issue with an alternating arrangement of slits and wells, the so-called slit-well (SW) motif, in silicon and demonstrated separation of biomolecules over a broad size range [9]. Yet, a high-strength field ($\geq$100 V/cm) that is often required for fast separation had the separation mechanism break down and led to a poor separation. Recently, Cao *et al*. replaced slits with arrays of capillaries, the capillary-well (CW) motif and demonstrated that the separation in such design takes place at a high voltage, rapidly resolving macromolecules into sharp bands [10]. This was attributed to 2D confinement within capillaries as opposed to 1D confinement within slits and steep entropic barriers imposed on migrating molecules at a capillary entrance.

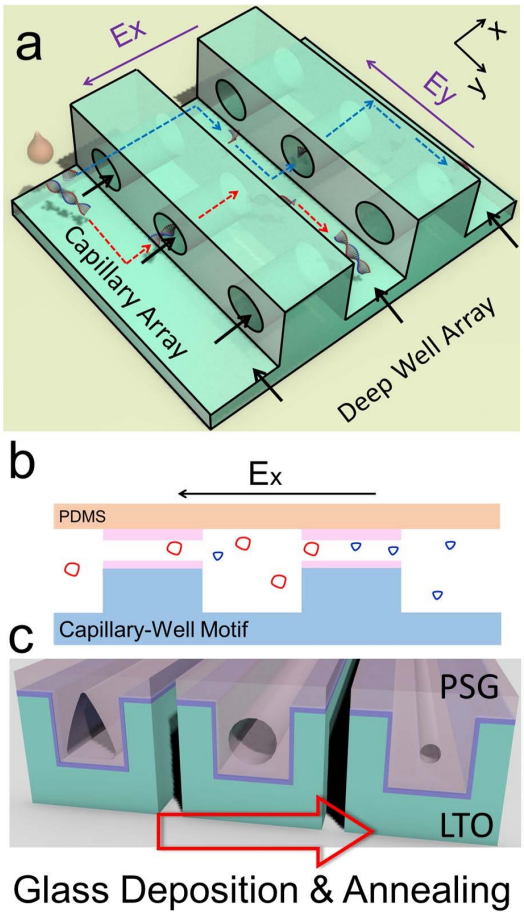

Figure 1: Illustrations: (a) CW array segment. (b) Ogston sieving description on a cutaway view along x direction. (c) Nanocapillary fabrication: glass deposition and reflow.

Here, we advance the CW motif from batch to continuous-flow separation. Figure 1a partially illustrates the CW motif. Negatively charged macromolecules being injected from a point under y -direction electric field, overcome entropic barriers based on their size and jump to adjacent wells under x-direction field. This causes the input to split into streams with each stream delivering macromolecules of a specific size deflected accordingly. Since the capillary diameter is larger than macromolecules of interest, the Ogston regime prevails here with smaller macromolecules deflecting at a greater angle than larger ones, Figure 1b. The CW motif consists of wells and capillaries fabricated by a unique process described in Figure 1c. The capillaries are self-enclosed conduits formed by phosphosilicate glass (PSG) deposited in trenches etched within a low-temperature oxide (LTO) layer and then turned into cylindrical tunnels under shape transformation through thermal annealing [11]. The thermal annealing duration was extended to controllably shrink the capillary diameter down to 100 and 600 nm for sieving protein mixtures and DNA mixtures, respectively.

MATERIAL AND METHODS

Fabrication

Major fabrication steps are illustrated in Figure 2. The structures were fabricated into a 6-µm thick LTO layer placed on p-type silicon wafers <100> oriented, and 4-inch diameter using plasma-enhanced chemical vapor deposition (PECVD). Prior to LTO deposition, the wafers were thermally oxidized growing an insulation layer 1 µm thick, Figure 2a. Subsequently, trenches 2 µm wide and deep were etched into the LTO layer using reactive ion etching (RIE), followed by a deposition of low-stress nitride (LSN) 100 nm thick as a diffusion barrier, Figure 2b. PSG layer was then deposited 5.5 µm thick through low-pressure CVD (LPCVD, 180mTorr), forming self-enclosed voids extending along trenches, Figure 2c. These voids were transformed into cylindrical capillaries 750 nm in diameter through thermal reflow (1000 °C, 60 min). Chemical mechanical polishing (CMP) was then applied to flatten the surface and reduce the thickness of PSG layer down to ~2 µm. Subsequently, microfluidic access channels were structured through RIE along with deep wells partitioning the capillaries, Figure 2d. The wells were etched 2 µm deep and wide and interleaved with arrays of capillaries 2 µm long (pitch 4 µm). The rapid thermal annealing (RTA) was performed for controlled scaling of the capillary diameter down to 600 or 100 nm. Lastly, a polydimethlysiloxane (PDMS) slab punched with inlet/outlet ports was bonded on the substrate after surface activation in oxygen plasma.

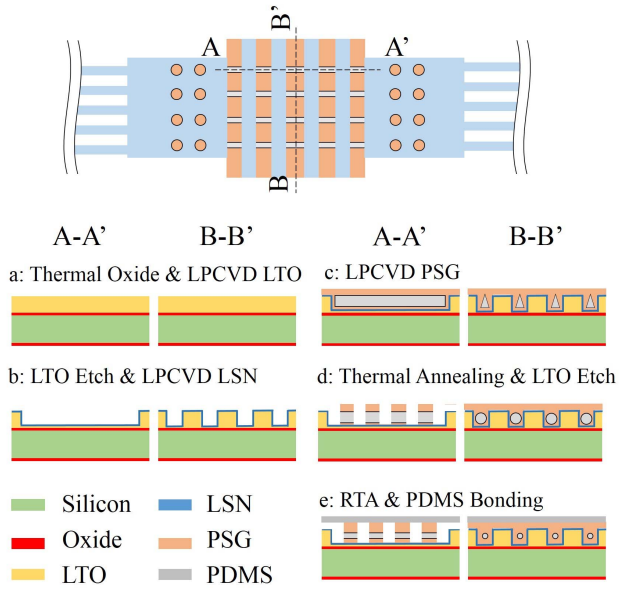

Figure 2: Major fabrication steps illustrated on substrate cross-sectional profile (longitudinal: A-A' and transverse: B-B' cutaway views as denoted in layout in upper panel).

Reagents

Double-stranded DNA (dsDNA) fragments with chain length of 5 and 10 kbp, intercalating dye YOYO-1, Alexa Fluor 488 conjugated proteins, including cholera toxin subunit B (11.4 kDa) and ovalbumin (45 kDa), were purchased from Thermo Fisher Scientific (Waltham, MA); Ethylenediaminetetraacetic acid (EDTA), sodium dodecyl sulfate (SDS), and dithiothreitol (DDT) were acquired from Sigma-Aldrich (St. Louis, MO); Tris and borate were obtained from Sigma chemicals Co. (St. Louis, MO). All the dsDNA samples were labelled with YOYO-1 at a dye/base pair ratio of 1:10 and dissolved at a concentration of 50 µg/mL into 5× TBE buffer (445mM Tris/borate, 10mM EDTA, pH ~8.3). The proteins were mixed with %2 wt SDS and 0.1 mM DDT, and incubated in a water bath at 80 °C for 10 min. The resultant protein mixture was further diluted with 5 × TBE buffer to a final concentration of 0.2 mg/mL.

Experiments

The sieving structure was primed with 5× TBE buffer. In all experiments, the dsDNA and SDS-denatured proteins migrated along the direction of electrophoresis. To provide the electric fields, platinum electrodes (Leego Precision Alloy) with one end immersed in the reservoirs were connected to a high-voltage power supply (Tianjin Dongwen Co. Ltd.). The experiments were observed through an epi-fluorescence microscope (Eclipse, Nikon, Tokyo, Japan) and the images were captured with a thermoelectrically cooled EMCCD camera (iXon3897, Andor). A 100 W mercury lamp (Nikon, Tokyo, Japan) was used for illumination and a filter cube set (Ex/Em: 491/509 nm, YOYO-1; 495/518 nm, Alexa Fluor 488) was used to observe the fluorescent streams. The images were analyzed by an image processing software (Image J, NIH, Bethesda, MD). The electropherograms were obtained by extracting and plotting the fluorescence intensities from regions of interests ~2 µm wide (denoted by dashed lines). The peaks were fitted with a Gaussian function to acquire the parameters, including the mean (at the maximum intensity), and width of respective streams (OriginPro 8.5, OriginLab Corp., Northampton, MA). Resolution was evaluated $R_s = 0.5 \times (x_1 - x_2)/(\sigma_1 + \sigma_2)$ where x_i and σ_i refer to the mean and standard deviation of the respective stream. Due to the limited signal to noise ratio, the resolution at the bottom can only be calculated by linearly extrapolating the stream width and separation distance along the streams.

RESULTS AND DISCUSSION

2D CW motif

Figure 3 depicts the scanning electron micrographs of the fabricated CW motif closing on specific sections of the motif as indicated on the device layout schematic in Figure 3a. Also illustrated on the layout schematic is the electrical wiring configuration during device operation. Figure 3b focuses on microfluidic channels surrounding the motif that ensure uniform electric field through the current-injection method. Figure 3c and 3d respectively shows the sample channel for the continuous injection of a mixture of macromolecules into the motif and the sample collection ports at the other end for the retrieval of size-fractionated streams. The shown motif features a fine pitch of 4 µm between wells and arrayed nanocapillaries equally divided. Figure 3e reveals a close-up view of the nanocapillaries with diameter of 600 and 100 nm for DNA and protein sieving, respectively.

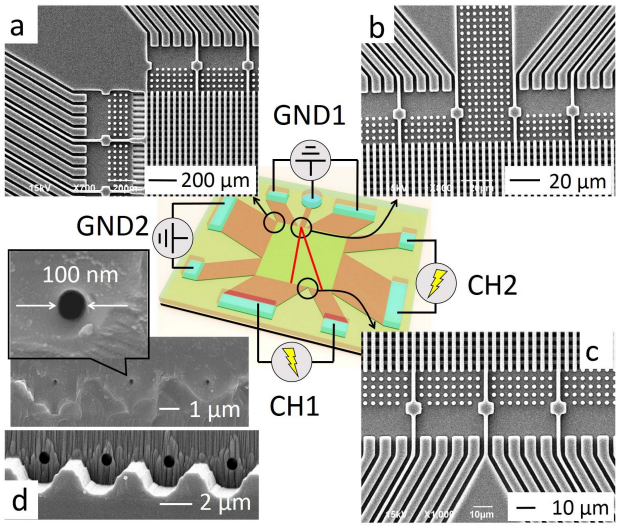

Figure 3: (a) Device rendering with electrical connections as illustrated. Images depicting channels for (b) buffer (c) sample input and (d) fractionated sample outputs all connected to respective reservoirs at the periphery. (e) Images of the capillary openings used for sieving proteins (upper panel) and DNA chains (lower panel).

Continuous-flow DNA separation

To demonstrate the sieving of dsDNA in the Ogston regime, we used a binary mixture of 5 and 10 kbp DNA and a 600-nm CW motif with the capillary diameter larger than the gyration radii of the fragments, 173 and 245 nm, respectively. The fragments were injected into the motif following electrophoresis under an electric field applied along y axis at a strength E_y. When superimposed with an orthogonal field applied at a strength E_x, the chains were observed to fractionate based on their size by overcoming entropic energy barriers between wells across the motif. In Ogston sieving, short chains overcome these barriers more rapidly than long chains and migrate at a comparatively high mobility. Therefore the stream of short chains exhibits a comparatively large deflection angle because of the smaller distance traveled along deep well between two consecutive capillary crossings.

Figure 4 presents fluorescent micrographs depicting the size fractionation of DNA fragments through the motif under two distinct field strengths E_x~ 100 and 200 V/cm. The dashed lines on the images denote the axes along which the fluorescent intensity plots are given. We notice that the stream deflection angles as well as dispersions increased with the increased electric field strength E_x. Specifically, at E_x~200 V/cm an enhanced baseline resolution R_s~0.96 is noticeable as compared to R_s~0.62 the value at E_x~100 V/cm. An increase in E_x and E_y leads to improved resolution and faster separation speed, respectively. Therefore, a careful modulation of these orthogonal fields potentially brings rapid separation without degrading the resolution. Figure 4d quantitatively plots the stream deflection angle as a function of E_x for both DNA fragments 5 and 10 kbp. The plot reveals that the deflection angle increases with E_x as the molecules are driven over the entropic barriers at an increased mobility.

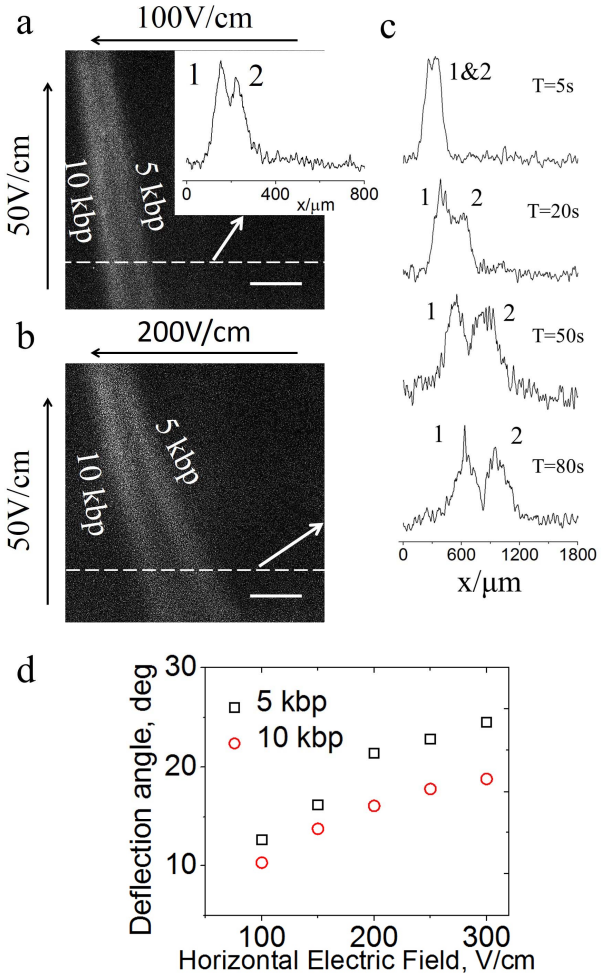

Figure 4: (a,b) Fluorescent images depicting the size fractionation of 5 and 10 kbp DNA in 600-nm CW motif captured around the exit region (Figure 3d) under two distinct electric field protocols. (c) Corresponding time-stamped fluorescent intensity plots illustrating baseline separation. (d) Deflection angle measured as a function of the field strength in x-direction with the field strength in y-direction being fixed at 50 V/cm. Peak assignments: (1) 10 and (2) 5 kbp. Scale bar: 400 µm.

After verifying the dependence of deflection angle on the horizontal electric field, we explored the separation performance with respect to the time and spatial scale by plotting electropherograms. As shown in Figure 4c, the time-stamped plots indicate how fast the separation occurs upon voltage onset; it takes ~80 s to baseline resolve two chains after a maximum migration distance ~1.5 mm along x-direction. In comparison, by applying a SW motif in the Ogston regime, Fu and colleagues achieved a baseline separation of short DNA fragments within ~2 min after a migration distance ~2 mm [9]. Therefore, our CW motif delivers continuous-flow fractionation of macromolecules at a comparable resolution by using a comparatively small array size and fast separation time.

Continuous-flow SDS-denatured protein separation

We also investigated the size fractionation of proteins under denaturing conditions. A binary mixture of SDS-denatured proteins constituting cholera toxin subunit B (11.4 kDa) and ovalbumin (45 kDa) was injected into a 100-nm CW motif. As shown in Figure 5a, the proteins became fractionated according to Ogston sieving with cholera toxin subunit B deflected at a greater angle (~26.4°) than ovalbumin (~14.6°). The corresponding fluorescent intensity plot indicates a separation resolution of ~1.5 along the dashed line situated at a distance 2.5 mm from the injection point, Figure 5b. The resolution further increases and becomes ~2.6 (extrapolated) at the exit of the CW motif.

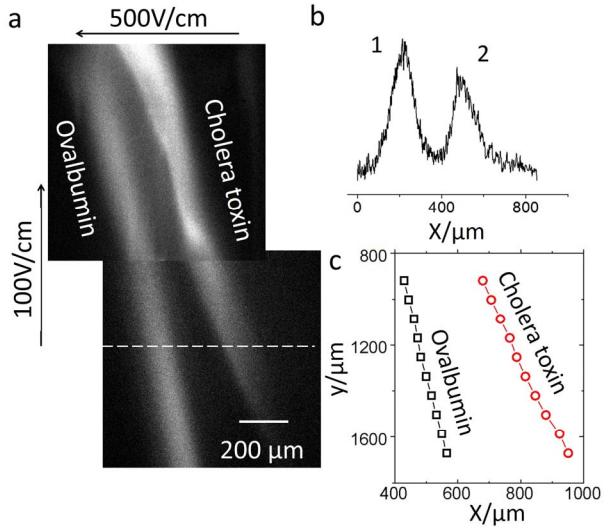

Figure 5: (a) Fluorescent images depicting fractionation of SDS-denatured proteins including cholera toxin subunit B (11.4 kDa) and ovalbumin (45 kDa) captured around the exit in 100-nm CW motif. (b) Corresponding intensity plot with peak assignments as (1) ovalbumin and (2) cholera toxin subunit B. (c) Measured protein trajectories in reference to peak fluorescence intensity levels.

CONCLUSION

We have demonstrated continuous-flow fractionation of biological macromolecules through a 2D CW motif in the Ogston regime. This novel design features thousands of glass nanocapillary segments in cylindrical profile and integrated through low-resolution photolithography (~2 µm) and standard silicon micromachining techniques. Both DNA fragments and proteins have been fractionated based on size in 600- and 100-nm devices, respectively. Compared to the conventional SW motif, the CW motif presents sharply increased entropic barriers owing to increased order of confinement within the capillaries. Therefore, the use of highly restrictive capillaries reduces the required sieve matrix size and overall separation time. Given its high performance and compatibility with standard semiconductor manufacturing settings, the CW motif holds a great potential as a stand-alone artificial sieving matrix as well as a module to be integrated within a fully automated biomolecule separation and analysis microsystem.

ACKNOWLEDGEMENTS

This project was financially supported by the Research Grant Council of Hong Kong under GRF 621513.

REFERENCE

[1] K. D. Dorfman, S. B. King, D. W. Olson, J. D. P. Thomas, and D. R. Tree, "Beyond Gel Electrophoresis: Microfluidic Separations, Fluorescence Burst Analysis, and DNA Stretching," *Chemical Reviews,* vol. 113, pp. 2584-2667, Apr 2013.

[2] J. L. Viovy, "Electrophoresis of DNA and other polyelectrolytes: Physical mechanisms," *Reviews of Modern Physics,* vol. 72, pp. 813-872, Jul 2000.

[3] J. Y. Han, J. P. Fu, and R. B. Schoch, "Molecular sieving using nanofilters: Past, present and future," *Lab on a Chip,* vol. 8, pp. 23-33, 2008.

[4] W. D. Volkmuth and R. H. Austin, "DNA Electrophoresis in Microlithographic Arrays," *Nature,* vol. 358, pp. 600-602, Aug 13 1992.

[5] S. Rahong, T. Yasui, T. Yanagida, K. Nagashima, M. Kanai, A. Klamchuen*, et al.*, "Ultrafast and wide range analysis of DNA molecules using rigid network structure of solid nanowires," *Scientific reports,* vol. 4, p. 5252, 2014.

[6] J. Han and H. G. Craighead, "Separation of long DNA molecules in a microfabricated entropic trap array," *Science,* vol. 288, pp. 1026-1029, May 12 2000.

[7] L. R. Huang, J. O. Tegenfeldt, J. J. Kraeft, J. C. Sturm, R. H. Austin, and E. C. Cox, "A DNA prism for high-speed continuous fractionation of large DNA molecules," *Nature Biotechnology,* vol. 20, pp. 1048-1051, Oct 2002.

[8] Y. Zeng, M. He, and D. J. Harrison, "Microfluidic self-patterning of large-scale crystalline nanoarrays for high-throughput continuous DNA fractionation," *Angewandte Chemie-International Edition,* vol. 47, pp. 6388-6391, 2008.

[9] J. P. Fu, R. B. Schoch, A. L. Stevens, S. R. Tannenbaum, and J. Y. Han, "A patterned anisotropic nanofluidic sieving structure for continuous-flow separation of DNA and proteins," *Nature Nanotechnology,* vol. 2, pp. 121-128, Feb 2007.

[10] Z. Cao and L. Yobas, "Gel-Free Electrophoresis of DNA and Proteins on Chips Featuring a 70 nm Capillary-Well Motif," *Acs Nano,* vol. 9, pp. 427-435, Jan 2015.

[11] Y. F. Liu and L. Yobas, "Cylindrical glass nanocapillaries patterned via coarse lithography (> 1 mu m) for biomicrofluidic applications," *Biomicrofluidics,* vol. 6, Dec 2012.

CONTACT

*L. Yobas, tel: +852-2358 7068; eelyobas@ust.hk